UPTEC ES 23021
Examensarbete 30 hp
september 2023

UPPSALA
UNIVERSITET

Theoretical examination of temperature distribution in an electrical furnace by the study of transient heat conduction effects

Judith Bösenecker

Civilingenjörsprogrammet i energisystem

UPPSALA UNIVERSITET

Theoretical examination of temperature distribution in an electrical furnace by the study of transient heat conduction effects

Judith Bösenecker

Abstract

The company Kanthal produces electric heating elements that require high temperature treatment in one production step. In this process step, called sintering, the amount of heat received by the sintered material is in direct correlation to the product's outcome.

It is therefore of interest for the company to gather information about how heat transfer happens in an electrical furnace.

This study examines two different possible scenarios of how the heat transfer in the furnace could look like and which amount of heat the sintered material would receive. The relation between a gaseous ambience at a certain temperature and the temperature an object submerged into this ambience is assuming is studied in the process called "transient heat conduction".

Two models were built in Matlab, representing transient heat conduction effects on two different geometries: a plane wall and a short cylinder.

It could be shown that transient heat conduction effects turned out differently for the two models. The conclusion drawn from the results was that the wall model was susceptible to horizontal heat transfer effects, whereas the cylinder model was affected from all directions equally.

Further, an analysis of the heat transfer channels within the furnace revealed that the heat leakage through the furnace muffle edges, which are in contact with air, causes a multiple in heat loss compared to the overall heat leakage.

Teknisk-naturvetenskapliga fakulteten

Uppsala universitet, Utgivningsort Uppsala/Visby

Handledare: Petter Lindblom Ämnesgranskare: Ralph Scheicher

Examinator: Susanne Mirbt

Populärvetenskaplig sammanfattning

Företaget Kanthal är bosatt i Hallstahammar sedan 1931 och är specialiserad på elektriska värmeelement (Kanthal no date). Bland företagets produkter finns Kanthal ® Super, som innnebär ett utbud av keramiska värmeelement, vilka anses vara särskilt resistent mot oxidation under exponering för höga temperaturer (*Kanthal Super Electric Heating Elements handbook* 2022).

Kanthal ® Super används inom många storskaliga projekt runt om i världen. Ett exempel är projektet ELROS som är ett samarbete mellan olika företag och forskgningsavdelningar med målet att hitta lösningar på elektrifieringen av stålindustrin. Detta för att minska stålindustrins koldioxidutsläpp. (Kanthal 2021)

Råmaterialet för värmeelementen är i pulverform, som sedan i flera produktionssteg formas till en grön kropp. Till slut genomgår materialet sintringsprocessen, som initieras av exponering för höga temperaturer i en speciell ugn. Sintringen eliminerar porer vilket medför att materialet krymper ihop och blir mera tätt. (Carlström 2010)

Det är därför intressant att undersöka ugnens temperaturfördelning och hur en möjlig sådan skulle påverka det sintrade materialet.

Inom fysiken kallas fenomenet av objekt som utsätts för en tidsvariende omgivningstemperatur för "transient värmeledning"(Incropera et al. 2017). Med hjälp av denna fysikaliska teorin undersöktes materialets temperaturbeteende som respons till gasflödet som det exponerats för.

Situationen simulerades i Matlab för två teoretiska scenarion, där två olika geometrier representerar det sintrade materialet. Första modellen är tvådimensionell och föreställer en cylinder, andra modellen är endimensionell och föreställer en vägg. Resultaten demonstrerar hur värmetransfer från olika håll skulle i teorin påverkar materialet.

Utöver detta genomfördes en analys av ugnens "värmeledningskanaler" med syftet att identifiera källorna för värmeläkage. Analysen avslöjade att ugnsmufflerna läcker mycket värme.

Executive summary

An important step in the production of the ceramic heating elements by the company Kanthal is the sintering of the material. As this is a high temperature process, it requires special industrial furnaces with high demand for energy and accuracy in temperature control. It is therefore Kanthal's concern to gather detailed information around heat transfer within their furnaces. Accordingly, this report was written to examine how heat transfer works inside an electric furnace, with the focus laid on how the sintered material interacts with the heated gas ambience.

Two models have been built to simulate heat transfer from different directions and dimensions, where the two-dimensional model yielded an uniform temperature distribution along the material and the one-dimensional model showed spatial variations in temperature. The company is encouraged to consider the report results in their constant attempt to improve the process of production.

Furthermore, an analysis of so called heat transfer channels within an electric furnace was carried out. By means of the provided theory, the company could conduct future studies on electrical efficiency of their electric furnaces and detect heat leakages mathematically.

Contents

List of used expressions

$t = time\ step$

Theta: Dimensionless temperature

$$\theta_{cyl} = \frac{T(r,t) - T_\infty}{T_i - T_\infty} = A_1 e^{-\lambda_1^2 * \tau} = theta\ for\ long\ cylinder\ model\ for\ r = 0$$

$$\theta_{wall} = \frac{T(x,t) - T_\infty}{T_i - T_\infty} = \sum_{n=1}^{\infty} A_n e^{-\lambda_n^2 * \tau} * \cos\left(\frac{x}{L} * \lambda_n\right) = general\ wall\ model$$

$$\theta_{L_{wall}} = \sum_{n=1}^{4} A_n e^{-\lambda_n^2 * \tau} * \cos\left(\lambda_n\right) = theta\ for\ wall\ model\ for\ x = L$$

$$\theta_{0_{wall}} = \sum_{n=1}^{4} A_n e^{-\lambda_n^2 * \tau} = theta\ for\ wall\ model\ for\ x = 0$$

$$\theta_{L_{sc}} = \frac{T(L,0,t) - T_\infty}{T_i - T_\infty} = \theta_{cyl} * \theta_{L_{wall}}$$

$$\theta_{0_{sc}} = \frac{T(0,0,t) - T_\infty}{T_i - T_\infty} = \theta_{cyl} * \theta_{0_{wall}}$$

OBS: the coefficients A and λ are different for wall- and cylinder model. For the definition of the formula elements see appendix.

Power values

Variable	Meaning	Unit
$\dot{Q}_{tot}$	$theoretical\ total\ power$	[W]
$\dot{Q}_{in}$	Theoretical power from heating elements entering the furnace chamber	[W]
$\dot{Q}_1$	Shaft losses $\left(\dot{Q}_1 = \dot{Q}_{tot} - \dot{Q}_{in}\right)$	[W]
$\dot{Q}_{conv1}$	natural convection heat transfer from heating elements to furnace ambience	[W]
$\dot{Q}_{rad}$	Radiation from heating elements to furnace walls	[W]
$\dot{Q}_{walls}$	heat leakages through furnace sides	[W]
$\dot{Q}_{air}$	Theoretical power spent on heating up the furnace air	[W]
$\dot{Q}_{edge}$	heat leaking via one muffle edge	[W]

Heating elements (to heat the furnace)

Variable	Meaning	Unit
ε_{he}	$emissivity\ heating\ elements$	
L_u	$terminal\ length$	[m]
L_e	$heating\ zone\ length$ (one leg)	[m]
a	$shank\ distance$	[m]
L_h	$heating\ zone\ length$	[m]
A_{he}	$area\ heating\ zone\ of\ one\ heating\ element$	$[m^2]$
A_{hes}	$total\ area\ of\ all\ heating\ zones\ of\ all\ elements$	$[m^2]$

Material to be sintered

Variable	Meaning	Unit
α	$thermal\ diffusivity\ of ceramic\ material\ at\ average\ temperature$	$[\frac{m^2}{s}]$
k_m	$conductivity\ for\ of ceramic\ material\ at\ average\ temperature$	$[\frac{W}{mK}]$
ε_m	$emissivity\ of\ the\ material$	
L	$half-length\ of\ ceramic\ material$	[m]
r_m	$radius\ of\ half\ cylinder\ approximation$	[m]
T_l	$temperature\ at\ material\ end\ (where\ x = L)$	[°C]
T_0	$temperature\ in\ the\ middle\ of\ the\ material\ (where\ x = 0)$	[°C]

Inner furnace ambience

Variable	Meaning	Unit	Source
$T_{\infty 1}(t)$	$assumed\ inner\ furnace\ ambience\ temperature$		
$T_i(t)$	$calculated\ temperature\ of\ the\ inner\ oven\ walls\ inside\ the\ oven$	$[°C]$	
$T_{he}(t)$	Calculated temperature of the heating elements	$[°C]$	
c_v(t)	$isochoric\ specific\ heat$	$[\frac{J}{kg*K}]$	Literature values interpolated with Excel ("Prognose.linear") and converted to $[\frac{J}{kg*K}]$ (with molar mass of air= 0.02897 kg/mole)
ρ(t)	Density of air	$[\frac{kg}{m^3}]$	(Incropera et al, 2017), interpolated with Excel ("Prognose.linear")
$m_{air}(t)$	current mass of the air within furnace volume	[kg]	
$\Delta Q_{air}(t)$	Amount of heat used to heat up the furnace air for a particular time interval	[W]	

V	furnace volume	$[m^3]$	
$\Delta T_{air}(t)$	furnace air temperature rise within a particular time step	$[°C]$	
h_{nat}	Natural convection coefficient for air	10 $[\frac{W}{m^2K}]$	(Kosky et al 2021)
ε	$emissivity\ inner\ surfaces$		
F_{12}	view factor from heating elements towards furnace walls		
$T_o(t)$	$temperature\ of\ outside\ oven\ walls$	[°C]	
R_{wall}	$total\ conduction\ resistance\ of\ one\ wall\ side$	$[\frac{K}{W}]$	

Muffles

Variable	Meaning	Unit
h	$convection\ heat\ transfer\ coefficient\ from\ gas\ flow\ inside\ the\ muffle$	$[\frac{W}{m^2 * K}]$
k_{gas}	$conductivity\ for\ the\ gas\ at\ average\ temperature$	$[\frac{W}{mK}]$
D	$outer\ diameter\ of\ muffle$	[m]
d	$inner\ diameter\ of\ muffle$	[m]
$\dot{v}_g$	$gas\ volume\ flow\ for\ the\ gas\ inside\ the\ muffle$	$[\frac{l}{min}]$
V_{AVG}	$average\ velocity\ of\ gas\ flow$ $\dot{v}_g$, converted into $[\frac{m^3}{s}]$ and divided by $\pi * (\frac{d}{2})^2$	$[\frac{m}{s}]$
ν	$kinematic\ viscosity\ for\ the\ gas\ at\ average\ temperature$	$[\frac{m^2}{s}]$

Muffle edges

Variable	Meaning	Unit
A_{me}	Area muffle edge	$[m^2]$
k_{muffle}	Conductivity for the muffle	$[\frac{W}{mK}]$
T_{me}	Muffle thickness	[m]
k_g	conductivity of the gasket	$[\frac{W}{mK}]$
A_g	lower gasket area	$[m^2]$
T_g	gasket thickness	[m]
R_{edge}	total thermal resistance between gas inside the muffle and the outside of the muffle edges	$[\frac{K}{W}]$

Chapter 1

Background

Kanthal specializes in amongst others ceramic heating elements, where it has a leading position on the international market. One step in the production of Kanthal ® Super heating elements comprises the sintering of the material, where pores inside the material are eliminated by volume diffusion. The differences in surface energy causes the atoms to move closer together, when the material is heated (Richardson 2006). As a result of sintering the ceramic material shrinks in size, becoming more dense and more robust towards mechanical stress.

Today, Kanthal uses several different sintering furnaces. Some of them are heated with Kanthal's own heating elements. For better understanding of the sintering process within their own production, the company wishes to gain more knowledge about how temperature is distributed and transferred in one of the company's furnaces. The purpose of this thesis is to study the heat transfer within the furnace on a theoretical level with the use of mathematical models. The results from this study shall serve as an inspiration for the company as to which aspects about heat transfer are interesting to consider.

Limitations

The scope of this study is going to be limited to one furnace and one material class. Assumptions around shaft and roof losses as well as the interpretation of the measured effect values are based on the experiences of involved engineers and an electrician. This study assumes an well functioning temperature control system inside the furnace, without questioning possible damages or abrasion of its components.

Chapter 2

Theory: Thermal fluid analysis

Due to reasons of company secrecy, the furnace in question will neither be described in detail nor will any technical drawings be shown. For the sake of this thesis, it will suffice to know, that it consists of an insulated furnace chamber, heated with electric resistance heating elements, which are controlled via temperature sensors to hold a certain target temperature. The ceramic material is inserted into muffles, while being exposed to a gas flow through the muffles, which is needed for the process.

2.1 Gas flow in a pipe

In terms of fluid dynamics, the heating process of the ceramic material within the muffle can be compared to gas flow in a pipe. Pipe gas flow is a special case of forced convection. When heat is supplied onto the pipe surface from the outside, the fluid mean temperature changes while passing the pipe. This circumstance can be approximated by either constant surface heat flux or constant surface temperature, where in both cases the mean fluid temperature approaches the hot surface temperature in flow direction (Çengel, Turner, and Cimbala 2008, ch.19-6). This behaviour implicates colder gas ambience towards the muffle entrance. Still, it remains to be studied, how the material interacts with the presumably somewhat colder gas coming from the entrance.

2.2 Transient heat conduction

Whenever one examines objects with time-dependent temperature one deals with a phenomenon called transient heat conduction. In addition to time-dependency, spatial tempera-

ture variations inside an object can be studied. As soon as an object is subjected to a cooler or warmer ambience than its own temperature, convection heat transfer takes place at the objects' surface, that is the ambient gas or fluid starts to cool or to warm up the surface layer. Accordingly, a temperature gradient develops between the outer layer of the object and its inner layers leading to heat conduction inside the object. (see ch.18-1 Çengel, Turner, and Cimbala 2008)

2.3 The Biot number

For some objects with either a very small volume or a high heat conductivity this process happens so fast that one can in practice simplify it and assume uniform body temperature. If this is the case one speaks of a "lumped system analysis". A measure of whether this approach can be used is the Biot number (=Bi), a relation between the magnitudes of convection heat transfer at the body's surface and heat transfer into the object via conduction. For Bi below or equal to 0.1 one can always assume uniform body temperature. The higher Bi the more inaccurate the lumped system analysis becomes. (see ch.18-1 Çengel, Turner, and Cimbala 2008)

2.4 Short cylinder model

According to Incropera et al the Biot number is dependent of the object's geometry. 2.1 and 2.2 show the formulas for the Biot numbers for a long cylinder and a plane wall. It is to be noticed, that the formula for the long cylinder within some tables differs to the conservative form, were "r" is used instead of $\frac{r}{2}$ (Incropera et al. 2017).

$$Long \quad cylinder : Bi = \frac{h * \frac{r}{2}}{k} \tag{2.1}$$

$$Plane \quad wall : Bi = \frac{h * L}{k} \tag{2.2}$$

In the following, these two geometries represent two different models, which simulate the heating process of the ceramic material.
The one-dimensional cylinder model suggested by Çengel is the idea of a long cylinder, exposed to heat convection only along its long side (see chapter 18-2 Çengel, Turner, and Cimbala 2008). The ceramic material, however, even receives heat from the top and the bottom side, since it is completely submerged into the gaseous ambience. This adds a second

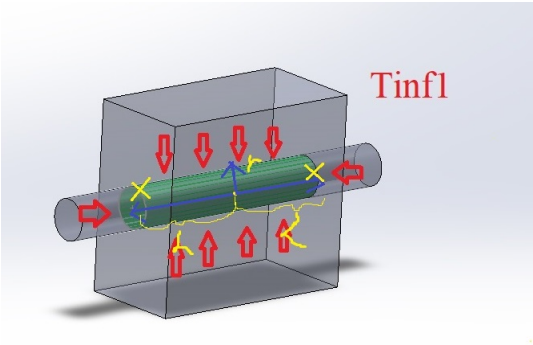

Figure 2.1: Model of the ceramic material as a composition of the geometries wall and cylinder

dimension to the problem. For multidimensional transient heat conduction, it is possible to consider an object as an intersection of different geometries that are exposed to the same surrounding fluid or gas temperature as long as there is no internal heat generation and that all sides are exposed to the same temperature T_∞ and share the same convection coefficient h. In that way, the ceramic material can be modelled as a "short cylinder", i.e. a long cylinder that is intersected by a wall (see figure 2.1). To combine the influences of transient heat conduction into radial and horizontal direction, a product solution can be used, multiplying the solutions for the wall and for the cylinder approximation, as will be explained later (see chapter 18-4 Çengel, Turner, and Cimbala 2008).

The Biot number for the wall model was determined as value and for the cylinder model it came out to be value (see appendix). It is to be noticed that for the cylinder model, the Biot number upon which the analytical solution to the transient heat conduction problem is built, is two times as big as the Biot number used to determine for or against the lumped system analysis, which was called the "conservative form" above (Biddle 2015).

For this concept to work, a uniform ambient temperature T_∞ is required from all sides.

2.5 Wall model

To show transient heat conduction effects into the horizontal direction only, the analysis can be reduced to one dimension. For this purpose, the ceramic material is regarded as a "wall" of thickness 2L that is exposed to an ambient temperature $T_{\infty 2}$ towards both sides (see figure 2.2). Height and width of the wall are assumed to be larger than its thickness to simulate one-dimensional heat transfer. (see chapter 18-2 Çengel, Turner, and Cimbala 2008)

Notice that in doing so, we disregard from the fact that heat is constantly supplied along the

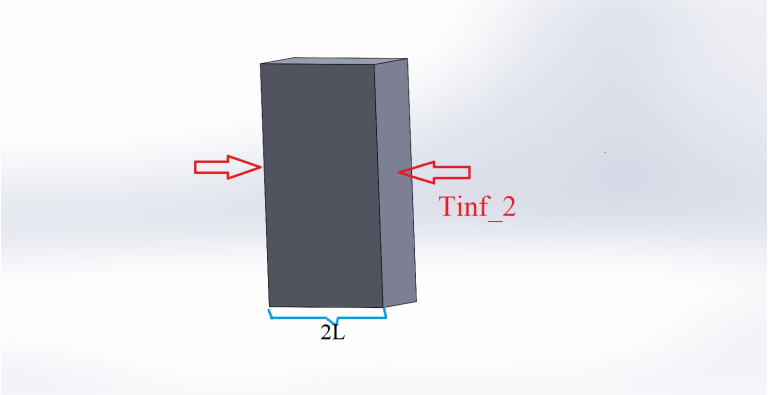

Figure 2.2: Model of the ceramic material as a wall

length of the material (into the vertical direction in figure 2.2), creating a much higher T_∞ in the middle of the furnace than at its edges. In reality, the middle part of the material will always be at higher temperature than the edges, whereas in our model heat is only supplied towards the edges, assuming a cold middle part. What is being simulated as a pure heating process, might in fact be a cooling process, with heat from the middle part escaping towards the cooler edges. But regardless from the direction of heat transfer, the pattern of $T_{\infty 2}$'s influence on the material's edges can be captured. In reality, it is assumed that neither of the processes is governing, but that as t goes towards infinity a steady state will be established between a hot middle part and a slightly cooler part at the edges.

The ambient temperature within the edges of the muffle will in the following be called $T_{\infty 2}$ and all other ambient temperatures towards the furnace's middle part will be denoted as $T_{\infty 1}$ to avoid confusion.

Chapter 3

Theory: Transient heat conduction equation: Analytical solution θ

The one-dimensional heat conduction problem can be stated in terms of nondimensionalized quantities and its solution is an infinite series, which differs for different geometries. Due to nondimensionalization the wanted temperature at a certain position along the material and at a certain time appears within the dimensionless temperature θ, a relation between all the different temperatures involved. Therefore, θ has in a final step to be solved for the desired temperature. For a plane wall the analytical solution is given in equation 3.1, where T_∞ stands for the temperature of the surrounding gas, T_i for the initial and uniform temperature of the object, A_n and λ_n are constants that depend on the Bi number, $\frac{x}{L}$ is the dimensionless position within the "wall" and τ is the dimensionless time of exposure and is also called the Fourier number. More details on how A_n, λ_n and τ are evaluated can be found in the appendix. The partial of temperatures in 3.1 and all following transient heat conduction formulas will be denoted as "temperature fraction", whereas the right-hand side will be called θ. (see chapter 18-2 Çengel, Turner, and Cimbala 2008)

$$\theta_{wall} = \frac{T(x,t) - T_\infty}{T_i - T_\infty} = \sum_{n=1}^{\infty} A_n e^{-\lambda_n^2 * \tau} * cos\left(\lambda_n \frac{x}{L}\right) \tag{3.1}$$

As it turns out, with the dimensionless time $\tau > 0.2$ a one-term approximation of the analytical solution can be used, where the error stays below 2 % (see chapter 18-2 Çengel, Turner, and Cimbala 2008).

When the cylinder model is applied, the dimensionless time τ turns out to be value, which

makes it possible to use the one-term approximation. Also, the only radial position of interest is the temperature at the cylinder's center. The dimensionless temperature θ for the cylinder model was then obtained by 3.2

$$\theta_{cyl} = \frac{T(r=0,t) - T_\infty}{T_i - T_\infty} = A_1 e^{-\lambda_1^2 * \tau} \tag{3.2}$$

Note, that the numerical values for the coefficients A and λ in 3.2 are different from those in 3.1, as they are based on different Bi numbers.

Looking on the transient heat transfer in horizontal direction, i.e. applying the wall model (see 3.1), τ only amounts to value, which makes the one-term approximation an insufficient solution. Still, it can be shown, that including only four terms gives a solution with satisfying accuracy.

A more detailed explanation of the formula's components can be found in the appendix.

For the sake of comparison of the temperature development at two different positions, the same iteration has been conducted for the position x=0 (in the middle of the material) and x=L (at the end of the material). In case of the short cylinder model, the spatial variable r=0 is added as an input to T.

Equations 3.3, 3.4, 3.5 and 3.6 summarize the different versions of θ which later on shall be set equal to the temperature fraction and solved for the desired temperature (more details on how the formulas are used in the Matlab code will be given in the next chapter). 3.3 and 3.4 represent the one-dimensional wall model for the two positions x=L and x=0. For the two-dimensional short cylinder model a product solution was used as mentioned before. 3.5 and 3.6 show the product solution, again for the positions x=L and x=0, as suggested by Çengel.

(Çengel, Turner, and Cimbala 2008)

$$\theta_{L_{wall}} = \theta_{wall}(L) = \sum_{n=1}^{4} A_n e^{-\lambda_n^2 * \tau} * cos(\lambda_n) \tag{3.3}$$

$$\theta_{0_{wall}} = \theta_{wall}(0) = \sum_{n=1}^{4} A_n e^{-\lambda_n^2 * \tau} \tag{3.4}$$

$$\theta_{L_{sc}} = \frac{T(x,r,t) - T_\infty}{T_i - T_\infty} = \theta_{sc}(L,0) = \theta_{cyl} * \theta_{L_{wall}} \tag{3.5}$$

$$\theta_{0_{sc}} = \frac{T(x,r,t) - T_\infty}{T_i - T_\infty} = \theta_{sc}(0,0) = \theta_{cyl} * \theta_{0_{wall}} \tag{3.6}$$

3.1 Numerical values for θ

- For the Bi number value wall model, the correspondent constants λ and A for the first four terms in the series and with τ equal to value, $\theta_{L_{wall}}$ was calculated to 0.7866
- In the same manner, $\theta_{0_{wall}}$ was found to be 0.9995
- With τ equal to value and the Bi number equal to value cylinder model θ_{cyl} turned out to be 0.012

(see appendix)

Chapter 4

Method: Matlab model

4.1 Transient heat conduction equation: temperature fraction

Next, the temperature fraction of the transient heat conduction equations was then together with θ to be solved for the wanted temperature of the ceramic material at the respective time and position in Matlab. At this point, however, another problem arose: Within all transient heat conduction formulas, which have been presented so far, the ambient gas temperature T_∞ appears as a constant. As a matter of fact, neither the furnace temperature nor the applied effect to the heating elements is constant over time, which makes T_∞ a time-dependent variable. The temperature fraction of the transient heat conduction formulas has therefore to be evaluated numerically at small time steps, for which T_∞ can assumed to be constant. For the temperature data test vectors have been used as T_∞, which simulate a heating process. The initial temperature T_i is then equal to the temperature T(x,t) from the previous calculation step at the respective position x (in the short cylinder model the spatial variable r is added, but it is always equal to zero).

The problem of time-dependency applies not to θ: All time steps are taken of equal length, so that τ, which only depicts the time of exposure to a certain constant temperature value, stays a constant. Thus, θ only depends on the position across the ceramic material as illustrated in 3.3, 3.4, 3.5 and 3.6.

The iteration through the eigtheen different time steps can be represented as the following:

$$for\ i = 1\ : T(x,t) = T_i(x,0) = room\ temperature \tag{4.1}$$

$$for\ i = 2:18\ : T(x,t) = \theta * (T_i(x,t) - T_\infty(t)) + T_\infty(t) \tag{4.2}$$

where

$$T_i(x,t) = T(x, t(i-1)) \tag{4.3}$$

At this point, it should be mentioned, that this study places an emphasis on the comparison of transient heat conduction effects from different directions without claiming to calculate correct temperature values for the furnace. Therefore, test vectors could be used as temperature data instead of actual measurement data. Nevertheless, it was of interest to insert similar temperature data into both models to be able to compare the outcomes.

Whereas the short cylinder model examines the reaction to temperature exposure from multiple sides, the wall model isolates the horizontal direction for heat transfer.

Chapter 5

Results and discussion for the transient heat conduction models

5.1 Short cylinder model

In this section the results from the Matlab code for the short cylinder model are presented. Details on the overall Matlab model have been given in the previous chapter. The first code part solves 3.5 and 3.6 for the temperature of the ceramic material at position x=0 and x=L respectively. When the two-dimensional short cylinder model was chosen to determine the dimensionless temperature θ and $T_{\infty 1}$ was assumed to be the surrounding gas temperature, the resulting temperature at the material ends (T(L,0,t)) and at its middle position (T(0,0,t)), was found to be as illustrated in figure 5.1. All temperatures almost coincide, therefore the three graphs appear as a single line. A closer look reveals, that both material temperatures are somewhat lower than the surrounding gas temperature and that there even is a slight temperature difference between the temperature at the material ends and the central position within the material, where the ends became slightly warmer. However, none of these differences is significant, as all temperatures are within at highest 1 °C apart from each other.

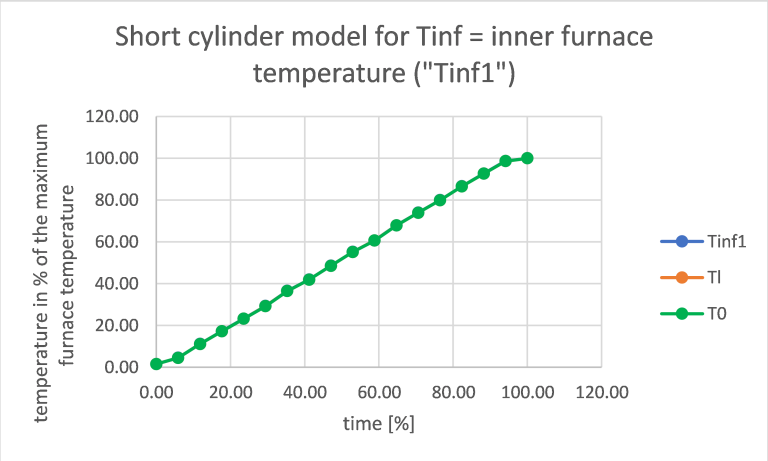

Figure 5.1: Resulting material temperature from the short cylinder model at different positions, compared to the surrounding gas temperature ($T_{\infty 1}$)

5.2 Discussion of the results from the short cylinder model

The results from the cylinder model displayed in figure 5.1 were not unexpected. Already, when the Bi number was calculated to be value cylinder model, it indicated that heat transfer in the radial direction would happen almost instantly. This was revealed to be true by the simulation results, since the material temperature approaches the ambient gas temperature very closely. Also, the temperature advance at the ends indicates, that they are slightly affected by the heat they receive from the "cylinder ends".

In practice, the result from figure 5.1 shows, that if the situation in the furnace would resemble the short cylinder model, where the ceramic material is exposed to an equal and uniform surrounding gas temperature $T_{\infty 1}$, then there would hardly be any difference in temperature experience along them. They would almost instantly assume a value close to the ambient gas temperature at all positions.

5.3 Wall model

Next, the results from the wall model are presented. The code is structured similarly to the one for the cylinder model, but now equation 3.1 is solved for the material temperature, again at central and end position, using the respective $\theta_{L_{wall}}$ and $\theta_{0_{wall}}$ from 3.3 and 3.4. Again, a test vector with temperature guesses for the gas temperature in the muffle edges ($=T_{\infty 2}$) was used for the wall model. It had the same pace in temperature increase as previously, but was chosen to be always somewhat lower then $T_{\infty 1}$ (the difference in $°C$ lies at 3% of the highest value of $T_{\infty 1}$). Figure 5.2 shows the results. The plot is again given in relative quantities, as percent of the respective highest occuring values.

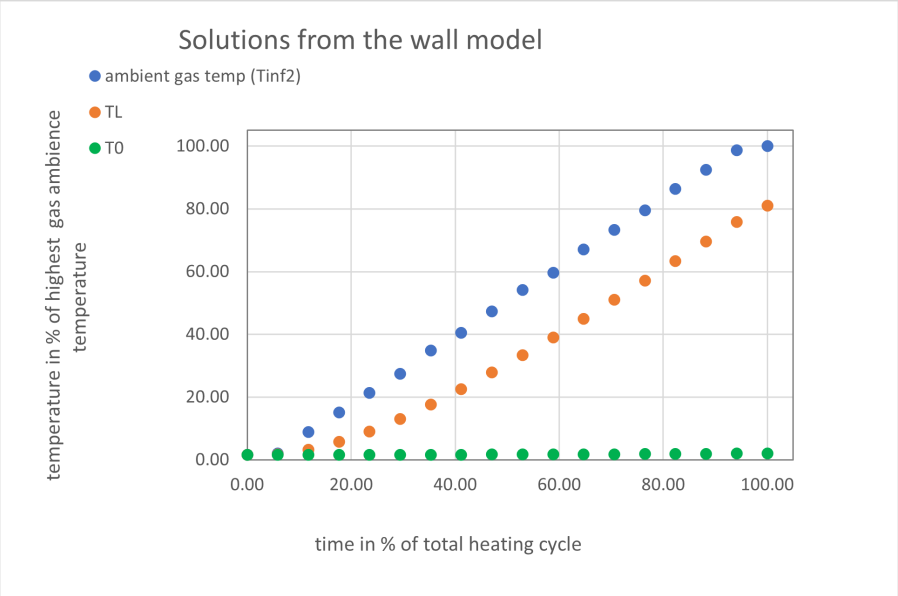

Figure 5.2: Results for the material temperature from the wall model for transient heat conduction with an assumed edge gas temperature of $T_{\infty 2}$=$T_{\infty 1}$ − 3%of the highest value

This time, there is a clear difference between all three temperatures displayed: The material's edge temperature clearly stays behind the temperature of the surrounding gas and the "wall center" at x=0 in the middle does almost not receive any heat at all.

The simulation has been run for another two test vectors with values for $T_{\infty 2}$ that were regarded to be extreme cases, one for extremely high and one for extremely low temperatures, but with the same shape of the heating curve as the original vector (see appendix). These extreme cases still yielded very similar results, only the mean temperature difference between the orange and the blue graph varied by a few degrees.

5.4 Discussion of the results from the wall model

Again, the results match the assumptions that could have been drawn from the Bi number: Its value of value wall model is well above the lumped system limit and so the model was expected to yield more significant effects of spatially variant transient heat conduction. At this point it is important to interpret the test results correctly since, as mentioned earlier, the mathematical model differs considerably from the reality. What has been modelled is a wall of ceramic material that is exposed to and heated by a certain gas temperature on both sides (see figure 2.2). In practice, instead of a "ceramic wall" the material receives heat from all sides.

The conclusion to be drawn from the results of the wall model is that a gas temperature $T_{\infty 2}$ within the edges of the muffle affects the material's temperature at different positions x differently strong: The outer edges closest to the edge temperature $T_{\infty 2}$ react rapidly on the temperature they are exposed to, even though they stay behind it. At the same time, the middle of the material hardly experiences any influence by $T_{\infty 2}$ at all.

For the real situation this reasoning implies the following: The wall model provides an insight in how the ceramic material is influenced by the temperature of the gas within horizontal direction towards them. In truth, there is no "wall of ceramics" that is blocking the gas flow from spreading over the entire length of the material. Instead, there is gas flow all over them. But, regardless of the heating process happening in radial direction, the wall model illustrates the consequences of temperature exposure towards the sides: Both, the material and the warm gas above it could be thought of as a "warm wall" exposed to a somewhat different temperature $T_{\infty 2}$ on both sides. Then, the material's temperature would be influenced strongly at x=L, but its effect would hardly be felt towards their center, at x=0, at all, as figure 5.2 shows.

If the gas temperature towards the inlet indeed should be cooler than in the middle of the muffle as anticipated in section 2.1, then the influence of the edge temperature might be a cooling rather than a heating effect (for $T_{\infty 1} > T_{\infty 2}$). According to the short cylinder model, the heat applied in the radial direction, warms the ceramic material quickly and exposure to a colder edge temperature would cool down material parts facing gas flow from the edges. In this way, the behaviour of heat transfer between the material's edges and its core part can assumed to be the same as for the simulated heating case: Whereas the edge region is affected by the edge temperature, the core part is not.

To obtain a more exact answer on which mechanisms of heat transfer take place inside the furnace and which temperature the material is thereof assuming requires a more complex model, involving the possibility for multiple surrounding ambience temperatures and at least

two transient heat conduction processes happening simultaneously. Such a setup demands a more advanced software like COMSOL® Multiphysics , dedicated to analyze complex models of heat transfer. For such an analysis, the actual gas temperatures $T_{\infty 1}$ and $T_{\infty 2}$ would have to be known.

5.5 Distinction between front- and backside

So far, equal convection conditions have been assumed to be present at both, front- and back side within the muffle. Although it is safe to assume that the heat transfer coefficient h is the same throughout the entire muffle, because there is only one value of gas flow, convection heat transfer is directed towards the "wall" only at the muffle's front side, according to the gas flow direction from front to back. Thus, the cooling effects from a colder edge temperature are valid for the material's side which is facing the inlet.

5.6 Discussion of radiation heat transfer effects

Another significant drawback of the of wall model is that the effect of radiation on the heat transfer coefficient h for forced convection inside the muffle was not considered. The convection coefficient h goes into the transient heat conduction calculations by determining the Bi number. Although Çengel mentions that radiation effects can be included into h (Çengel, Turner, and Cimbala 2008, see chapter 18-2), h only captures convection effects in this report. Nevertheless, one might argue, that radiation does not play a major role for the purpose of this study.

When it comes to the short cylinder model, the effects discussed above would only be enhanced, but not changed from radiation on the ceramic material from the muffle surface: Radiation in addition to the forced convection heat transfer would only make it more evident, that the material assumes ambience temperature instantly. Perhaps, the temperature differences between the ambience, the material end and its center would be eliminated completely. That is as long equal temperature from all heating elements is assumed, because then radiation affects all positions evenly.

As far as the wall model is concerned, its focus is on the thermal development at the edges of the muffle. Only a small part of the warm muffle surface extends beyond the material, i.e. outside the imaginary wall and into the area of impact for the wall model, to emit radiation onto the material's ends.

There is nevertheless another argument, that might be raised in the discussion around radiation: What about heat loss via radiation from the material towards the cold muffle edges?

The major part of the material is radiating heat back towards the warm area of the muffle. Since the muffle surface is at high temperatures already, no heat is lost via this transfer channel and the ceramic material emits about as much radiation as it receives.

At the same time, the material's edges facing in- and outlet of the muffle are emitting radiation, which is hitting the colder parts of the muffle surface. This radiation would be absorbed by the colder surfaces and invested in heating up those surfaces instead of being radiated back to the material, leaving them with a net heat loss. Anyhow, such a radiation loss would be proportional to the area of the material that is facing the colder surrounding, which is equal to the material's cross-section. Accordingly, the maximum of heat loss is obtained from the equation for net radiation from a surface (equation 21-39 Çengel, Turner, and Cimbala 2008, in chapter 21-7), when assuming zero back radiation and setting the material temperature to its theoretical max (= max temperature of the heating elements):

$$\dot{Q}_{loss} = \pi * r_m^2 * \epsilon_m * \sigma * T^4 \tag{5.1}$$

Here, $\pi * r_m^2$ stands for the material's cross section area, ϵ_m its emissivity and $\sigma = 5.67 * 10^{-8} \frac{W}{m^2 K^4}$ is the Stefan-Boltzman constant. Compared to the magnitude of other heat leakages the by 5.1 calculated amount is an insignificant number.

Chapter 6

Heat channel analysis

Apart from the examined effects of transient heat conduction a more general analysis of the overall heat transfer within the furnace has been conducted. In accordance with the report's aim to gain more knowledge about the heat transfer within the furnace, the following heat channel analysis is an important tool to understand the correlation of the electrical power input into the furnace and the resulting heating processes.

Figure 6.1 displays an overview over the different heat transfer channels, i.e. the possible ways, in which the inserted energy can travel. All intermediate forms of heat passing through are coloured pink, whereas the heat leaving the furnace is emphasized with different colours. In the following, these different channels of heat transfer are going to be explained. To explore them means to understand the furnace as an energy system and helps to detect possible shortcomings concerning the energy efficiency, such as heat leakages.

Furthermore, in the end of this analysis an example will be given of how to use the calculated heat flux to deduce a temperature value for the muffle edge temperature $T_{\infty 2}$ for the transient heat conduction model. This example is, however, serves only as an illustration of a possible application for the analysis, but is actually not suited for the calculation of actual temperature values, since too many approximations have been done and the heat channel analysis is highly sensitive towards inaccuracies. More on that in section 6.7.

The first law of thermodynamics states that energy cannot be created or destroyed during a process(Çengel, Turner, and Cimbala 2008, ch.3-6). Every Watt in electrical energy can therefore be allocated to one of the different energy transfer channels in its new form as heat flux. Next, it follows an attempt to break down the overall heat transfer within the furnace into different transfer channels.

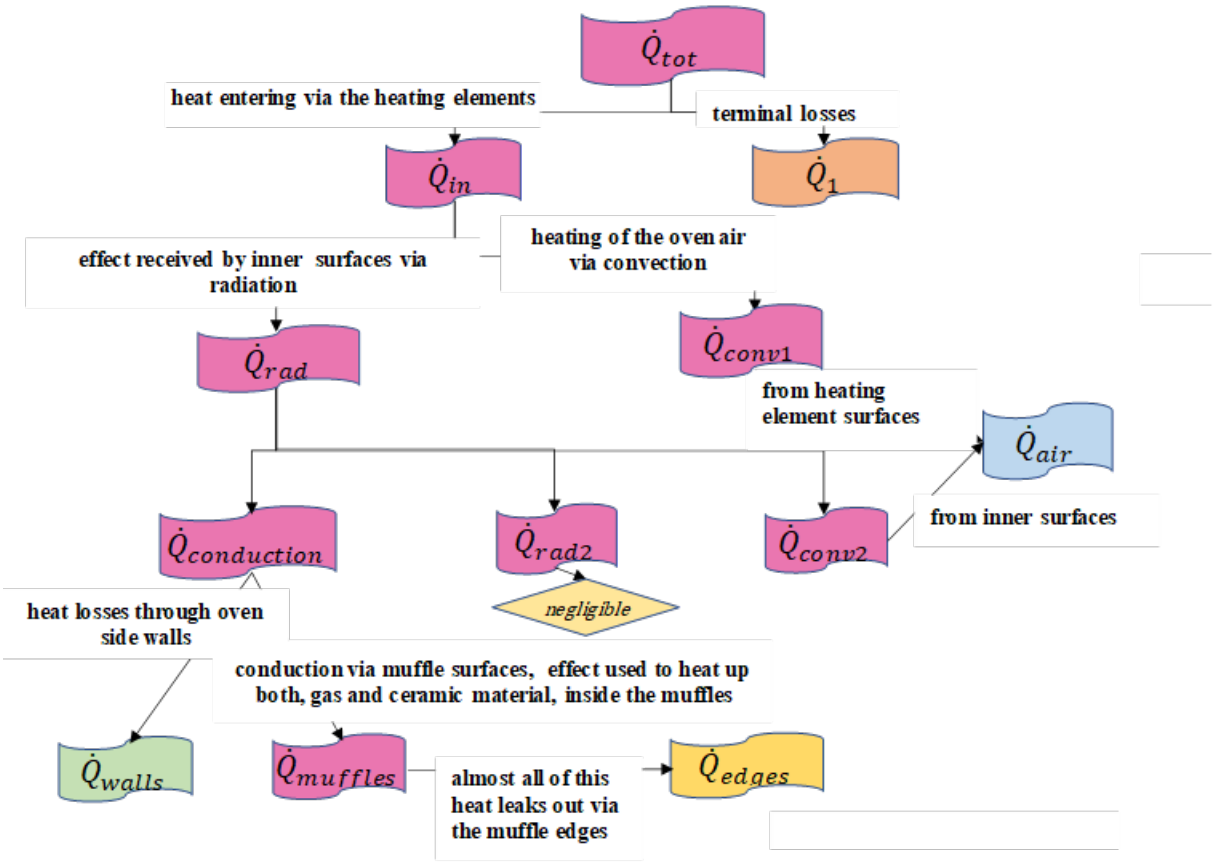

Figure 6.1: Overview on the different channels for heat transfer within the furnace

All temperature and power measurements which will be mentioned, should be conducted for a range of time steps throughout the heating process, if the thermodynamic development during the process is to be studied. It is recommended, to use the same time vector t as for the transient heat conduction analysis, if temperature data from the heat channel analysis is to be used as an input into the former (which is not recommended, unless a more detailed analysis is conducted, see 6.7).

6.1 $\dot{Q}_{in}$

At first, the electrical effect $\dot{Q}_{tot}$ is supplied to the heating elements. This total effect in [kVA] can be tracked in time by a computer linked to the furnace. It can be assumed that this amount in kVA corresponds to about the same amount in kW.

Furthermore, not the entire electrical power applied ends up as heat inside the furnace. A certain amount is heating up the terminals to the heating elements (L_u). With the help of a company-intern program, the amount of "terminal losses" for a certain instantaneous effect applied and a certain inner furnace temperature can be estimated and subtracted to obtain $\dot{Q}_{in}$.

$$\dot{Q}_{in}(t) = \dot{Q}_{tot}(t) - \dot{Q}_1(t) \tag{6.1}$$

6.2 $\dot{Q}_{conv1}$

From the heating elements inside the furnace, the applied heat can be transported further via either convection or radiation heat transfer. To calculate the amount of heat transferred by convection to the furnace environment, one needs the temperature of the heating elements (T_{he}) and the temperature of the air inside the furnace ($T_{\infty 1}$) at every time instance. The latter can be obtained from the computer, which apart from the electrical power even records temperature measurements of the furnace air. The company- intern program mentioned before can then be used to determine an element temperature T_{he}. Newton's law of cooling yields then the heat flux in [W] from the surface of the heating elements towards the surrounding furnace air as shown in 6.2 (Çengel, Turner, and Cimbala 2008, ch.20-3):

$$\dot{Q}_{conv1}(t) = h_{nat} * A_{hes} * (T_{he}(t) - T_{\infty 1}(t)) \tag{6.2}$$

For the natural convection coefficient h_{nat} a value of $10[\frac{W}{m^2 * K}]$ has been assumed as a common value for natural convection in air (Kosky et al. 2021, ch.14) and A_{hes} is the surface area of the heating elements (in the heating zone with length L_h).

6.3 $\dot{Q}_{rad}$

After subtraction of $\dot{Q}_{conv1}$ the remaining power was considered to be the radiation contribution $\dot{Q}_{rad}$ from the elements towards all inner furnace surfaces (see 6.3).

$$\dot{Q}_{rad}(t) = \dot{Q}_{in}(t) - \dot{Q}_{conv1}(t) \tag{6.3}$$

How $\dot{Q}_{rad}$ then is distributed over the inner furnace walls, is measured by the view factor, a geometric indicator of how much of a surface can be "seen" by the emitting object (Çengel, Turner, and Cimbala 2008, ch.21-4 and 21-7). Further, how much radiation thereof is absorbed by a surface is given by the surface's absorptivity (which in this case equals the surface's emissivity according to Kirchhoff's law).

If the view factor from the heating elements towards the inner surface walls is F_{12}, ϵ the surfaces' emissivity (heating elements and walls must have the same emissivity) and σ the Stefan-Boltzman constant ($=5.67 * 10^{-8} \frac{W}{m^2 K^4}$) ,then the surface temperature of the inner furnace walls can be calculated from equ.6.4 (equ. 21-45 in Çengel, Turner, and Cimbala 2008, ch.21-7). Note that, in order to simplify the calculations, the back radiation towards the heating elements was neglected, since their total surface area is of negligible size.

$$T_{inner}(t) = \left(T_{he}(t)^4 - \frac{\dot{Q}_{rad}(t)}{A_{hes} * F_{12} * \sigma * \epsilon_{sides}} \right)^{0.25} \tag{6.4}$$

It is to be noticed, that solving in this way for the inner wall temperature implies that the inner furnace walls are only being heated via radiation from the heating elements and not via convection from the inner furnace air. This assumption is justified if that the surfaces heated by radiation already are warmer than the furnace air.

6.4 $\dot{Q}_{walls}$

Despite the insulation, the main part of the generated heat inside a furnace is lost as leakage to the outside. In case of the furnace in question that means, heat is either leaking through the muffle edges, or via the furnace's side walls. It is assumed that no heat is leaking via the furnace's bottom. What further on is called $\dot{Q}_{walls}$ refers to heat leakage via the furnace side walls 3-6. To determine $\dot{Q}_{walls}$, the so called thermal network theory can be used to solve for the unknown quantity. Any heat flux between two or more mediums can be expressed as a ratio of the temperature drop and the thermal resistance between them. As Çengel et al show, these statements can be used to develop the thermal resistance network concept according to which the heat flux through a wall can be calculated, knowing the temperature on both sides of the wall and the thermal resistances of all mediums involved as illustrated in 6.5. (Çengel, Turner, and Cimbala 2008, ch. 17-1)

$$\dot{Q} = \frac{T_1 - T_2}{R_{tot}} \tag{6.5}$$

In order to calculate the amount of heat leakage through the furnace walls at a certain instance of time , one could measure the outside wall temperature (T_o) using a thermal camera , where the measurements have to be adjusted to the emissivity of the outside furnace walls. Then, 6.5 can be rephrased as in 6.6.

$$\dot{Q}_{wall}(t) = \frac{T_{inner}(t) - T_o(t)}{R_{wall}} \tag{6.6}$$

In 6.6, R_{wall} depicts the respective side wall's conduction resistance given by 6.7, where n is the amount of wall layers, L the layer's thickness in [m], k the material's thermal conductivity in $[\frac{W}{m*K}]$ and A_s the wall side's surface area in $[m^2]$. Values for thickness, surface area and conductivity of the individual insulation layers can be retrieved from technical datasheets.

$$R_{wall} = \sum_{i=1}^{n} \frac{L_i}{k_i * A_s} \tag{6.7}$$

This analysis should be done for each side wall individually, as outside surface temperatures T_o and the thermal resistances R_{tot} can differ for all four furnace walls regarded. In the following, the values for heat leakage from the furnace's side walls are called $\dot{Q}_3$, $\dot{Q}_4$, $\dot{Q}_5$ and $\dot{Q}_6$.

(Çengel, Turner, and Cimbala 2008, ch. 17-1)

6.5 $\dot{Q}_{air}$

One part of the generated heat is dedicated to warm up the air within the furnace ambience. As shown in figure 6.1 the inner furnace air is heated by natural convection from the heating elements as well as from the inner surface walls. Instead of adding all convection contributions, the total amount of energy going into heating up the air could be calculated in a more direct way. For every degree by which a certain mass of air molecules within a fixed control volume is heated, the amount of energy needed is described by the isochoric specific heat capacity c_v. This relation is expressed mathematically by 6.8 (Çengel and Boles 2011).

$$\Delta Q_{air}(t) = \dot{Q}_{air}(t) * s = m_{air}(t) * c_v(t) * \Delta T_{air}(t) \tag{6.8}$$

With the furnace temperature rising, the amount of moles of an ideal gas for a control volume of constant pressure decreases as does the air density, which again affects the total mass of air within the furnace (Çengel and Boles 2011). To obtain the momentary value for $\dot{Q}_{air}$ for the furnace temperature of the respective time step, the mass of air within the furnace volume can be calculated by

$$m_{air}(t) = \rho(t) * V \tag{6.9}$$

, where V is the inner furnace volume in $[m^3]$ and ρ is the density of air in $[\frac{kg}{m^3}]$ at the corresponding furnace temperature as interpolated values from (Incropera et al. 2017).

Likewise, interpolated values for the temperature-dependent isochoric specific heat capacity c_v of air at atmospheric pressure can be obtained from the literature.

For temperature increase ΔT_{air} the difference between one temperature measurement $T_\infty 1$ and the previous measurement can be taken for every time step.

6.6 $\dot{Q}_{edge}$

Finally, after having gathered all the information needed about the different heat channels through which energy is entering and leaving the furnace, one could solve for the heat leakage through the furnace muffles $\dot{Q}_{edges}$ as can be seen in 6.10.

$$\dot{Q}_{edges}(t) = \dot{Q}_{tot}(t) - \dot{Q}_{air}(t) - \dot{Q}_{wall}(t) - \dot{Q}_1(t) \tag{6.10}$$

6.7 $T_{\infty 2}$

In theory, the heat channel analysis, as described so far, can be used to deduce specific thermodynamic information about a certain part of the furnace. To illustrate that, an example will be given concerning the deduction of the inner muffle temperature $T_{\infty 2}$ towards the muffle's edges. Yet, this approach is highly sensitive to inaccuracies and should not be used, for a case like the furnace in this report, since too many approximations have been done. In a more elaborate study though, which is conducted with highly accurate temperature and power measurements and with the help of a multiphysics software, the presented method might give more acceptable results.

As before, the key method in solving for the wanted quantity is the thermal network theory, which was explained in the section concerning $\dot{Q}_{walls}$. This time, 6.5 is rephrased into 6.11, i.e. solved for $T_{\infty 2}$.

$$T_{\infty 2} = \dot{Q}_{edge} * R_{edge} + T_{o_{edge}} \tag{6.11}$$

6.7.1 $T_{o_{edges}}$

$T_{o_{edges}}$ is the outer surface temperature of the muffle's edges and the gasket, which again can be retrieved by the help of a thermal camera at different time instances (all temperature values for the muffle outside have to be adjusted to match the correct emissivity of the respective material). It is recommended to conduct measurements at different muffle spots and to do separate calculations for front- and backside of the furnace.

Only the overall value of heat loss $\dot{Q}_{edge}$ through the muffle edges is known from the above calculations. Therefore, an average of the different temperatures measured has to be assumed for respective edge on the front and on the backside of the furnace. Since the amount of heat flux through a surface is proportional to the area of the surface (see 6.6 and 6.7), the different temperature zones have to be weighted in correlation to how much area of exposure they contribute with.

6.7.2 R_{edge}

As in 6.6 the thermal resistance between the outside of the muffle edge and the inner muffle gas temperature can be regarded as a network of several resistances. Unlike before though, the requested temperature is the temperature of the surrounding gas inside the muffle, which adds another step of heat transfer, namely heat convection, into the calculations. The thermal resistance against heat convection can be included into the thermal network model with 6.12, where h is the convection heat transfer coefficient for the gas flow and A is the area of the surface subjected to heat convection (Çengel, Turner, and Cimbala 2008, ch.17-1). The derivation of h is part of the determination of the Bi number and can be found in the appendix.

$$R_{conv_e} = \frac{1}{h * A} \tag{6.12}$$

When it comes to the conduction resistance, the two different materials, the muffle material and gasket material, have to be taken into account. If one mentally cuts the muffle edge in

half and arranges its parts into a straight line, the combination of the gasket material and the muffle material material resembles a composite wall.

Çengel suggests to treat parallel heat conduction through a composite wall the same way as parallel electrical resistances (Çengel, Turner, and Cimbala 2008, ch.17-3):

$$\frac{1}{R_{eq}} = \frac{1}{R_1} + \frac{1}{R_2} = \frac{k_1 * A_1}{L_1} + \frac{k_2 * A_2}{L_2} \tag{6.13}$$

Replacing the indexed quantities in 6.13 by the properties of the the muffle material part and the others by the properties of the gasket, the total conduction resistance sums up to:

$$R_{wall_e} = \frac{1}{\left(\frac{k_{muffle} * A_{me}}{T_{me}} + \frac{k_g * A_g}{T_g}\right)} \tag{6.14}$$

Conductivity values should be taken at average process temperature. Together, R_{wall_e} and R_{conv_e} form the total resistance R_{edge} at the muffle edge.

At last, with all the necessary terms gathered, 6.11 could be solved to yield a theoretical $T_{\infty 2}$.

Chapter 7

Sources of Error

All calculations have been done for the properties of gas A, even though gas B has been used in the muffles instead for the two last hours of the heating cycle. If one wants repeat this study for the same furnace, the convection coefficient h should be calculated again for the thermal konductivity value of gas B, which also yields a new Bi number and different constants A and λ.

For the convection heat transfer coefficient, one calculates in general with an uncertainty around 15 % (Çengel, Turner, and Cimbala 2008, ch.18-1)

In all calculations the thermal properties of the materials and gases have been taken at an average temperature value, which is a common practice in the field.

Equal heating element temperatures were assumed at all times.

Furthermore, there are many sources of error coupled to the heat transfer channel analysis:

- Is the leakage via side 1 ($\dot{Q}_1$) only equal to the shaft losses? Or is more heat lost through holes within the roof?
- It was assumed that no heat was leaking through the bottom side.
- It has not been considered to test whether both convection contributions indeed add up to $\dot{Q}_{air}$
- $\dot{Q}_{edge}$ was assumed to be distributed equally among the muffle edges, independent of position.
- power measurements are expected to be fluctuating a lot. In order to use them, the

data has to be treated and simplified, be e.g. removing zero power points. The aspect of how to treat power data has not been spent any attention to and should be considered, if the heat channel analysis is to be used.

- The outside muffle edge temperature is treated as even by using an average value

Chapter 8

Conclusions and outlook

- The interaction of an ambient gas temperature and the ceramic material within the electrical furnace was studied with the theory of transient heat conduction. Two different geometries were chosen for the simulation to illustrate heat transfer from different directions and dimensions.
- The short cylinder model represented a case with uniform gas temperature from all sides. As a result, the material did not show any spatial differences during the heating process, but was heated up everywhere equally strong and it reached the ambience temperature instantly.
- In the wall model, the horizontal dimension of heat transfer was isolated and studied. Here, spatially varying heating effects could be identified, since the material's core part remained colder than the material's edges. Also, the edges never reached the same temperature as the ambience.
- An analysis of heat transfer channels within the electrical furnace has been provided. It has been shown, how temperature and heat leakage amounts at specific places within the electrical furnace could be deduced from electrical power input and easily accessible temperature measurements.

  One suggestion of how a future work could continue from this point is to determine the position, at which the material's temperature no longer is affected by the edge temperature $T_{\infty 2}$. This demands the iterative use of the wall model while the position x is gradually decreased, until the results for T_x do not change anymore with $T_{\infty 2}$.

  Moreover, the thermal network which was developed could be used in further exami-

nations of heat efficiency regarding the furnace. For this it is recommended though, to add more reliable data on bottom and top side of the furnace and to work with a high accuracy in temperature and power measurements. However, the heat channel analysis should be seen as an instrument to gather overall knowledge about the heat transfer within the furnace and is not suited for accurate calculations. For the latter, the reader is pointed to a multiphysics software like COMSOL® Multiphysics.

Appendix A

Details on fluid dynamic calculations

A.1 Heat convection coefficient h for pipe gas flow

All properties for gas A have been evaluated for an average temperature between room temperature (25°C) and maximum furnace air temperature. The values have been taken from (Cengel, Turner, and Cimbala 2008) and interpolated with Excel "Prognose.Linear". First, the Reynolds number has been calculated

$$Re = \frac{V_{AVG} * d}{\nu} \tag{A.1}$$

calculation of h

(Cengel, Turner, and Cimbala 2008)

A.2 The Biot number

A.2.1 For a long cylinder

Again, the thermal conductivity of the material has been taken for average temperature. Equation A.2 is for determining whether the lumped system analysis is applicable, according to Biddle (Biddle 2015), and A.3 is for calculating the coefficients for λ and A (Çengel, Turner, and Cimbala 2008, ch.18-2)

$$Bi = \frac{h * \frac{r_m}{2}}{k_m} = \text{value} \quad [dim. - less] \tag{A.2}$$

$$Bi = \frac{h * r_m}{k_m} = \text{conservative value} \quad [dim. - less] \tag{A.3}$$

A.2.2 For the wall

$$Bi = \frac{h * L}{k_m} = \text{value} \quad [dim. - less] \tag{A.4}$$

(Çengel, Turner, and Cimbala 2008)

A.3 The Fourier number (τ)

The dimensionless time τ, even called the Fourier number is for the two different geometries given by A.5 and A.6. In A.5 r_m is the radius of the cylinder and in A.6 L is the half-length of the wall. For the time t the amount of the time interval in [s] is inserted, which equals the time during which the material is exposed to a certain constant T_∞, whereas α depicts the material's thermal diffusivity in $[\frac{m^2}{s}]$ at average temperature.

A.3.1 For the long cylinder

$$\tau = \frac{\alpha * t}{r_m^2} = \text{value} > 0.2 \quad [dim. - less] \tag{A.5}$$

A.3.2 For the wall

$$\tau = \frac{\alpha * t}{L^2} = \text{value} < 0.2 \quad [dim. - less] \tag{A.6}$$

(Çengel, Turner, and Cimbala 2008)

A.4 The coefficients A_n and λ_n

A.4.1 For the wall

For the wall model the constant λ_n is given as root to the characteristic equation A.8 for each period π of this periodic function. Equation A.7 shows the formula for the constant A in the

wall model. In order to find λ's and A's corresponding to the respective period of π, Matlab was used. A program was written to calculate lambda for different intervals of multiples of π, including a function defining the Bi number as A.8.

Afterwards, another program solved for the wanted temperature in 3.1 at middle and end position, while calling functions to solve for 3.3 and 3.4 respectively. Results from the function calls for the wall model are displayed in table A.1. With the resulting θ for n=5 being negligibly low, only the first four terms were included into the sum of θ. When summing up the first four terms, $\theta_{L_{wall}}$ equals 0.7866 and the resulting $\theta_{0_{wall}}$ becomes equal to 0.9995.

$$A_n = \frac{4 * sin(\lambda_n)}{2 * \lambda_n + sin(2 * \lambda_n)} \tag{A.7}$$

$$\lambda_n * tan(\lambda_n) = Bi \tag{A.8}$$

(Çengel, Turner, and Cimbala 2008)

n	A	λ	$\theta_{L_{wall}}$	$\theta_{0_{wall}}$
1	A1	λ1	0.689	1.0863
2	A2	λ2	0.0897	-0.0941
3	A3	λ3	0.0076	0.0077
4	A4	λ4	0.0003807	-0.00038
5	A5	λ5	0.0000096	0.0000096

Table A.1: Coefficients (censored) for the wall model with Bi= value wall model and τ= value wall model and results for the dimensionless temperature θ at x=L and at x=0

A.4.2 For the long cylinder

The high Fourier number (τ) for the cylinder model, enabled the one-term approximation, where only the first λ and A were needed. To obtain the coeffients for long cylinder model, the values from table 18-2 in (Çengel, Turner, and Cimbala 2008) were interpolated to yield the corresponding values for Bi= conservative value . Another function in Matlab solves for equation 3.2. Table A.2 shows the numerical results and the solution for equation 3.2.

A.4.3 Product solution

Finally, the product solutions for the short cylinder model (see equation 3.5 and 3.6) are derived and presented in A.3. On the basis of $\theta_{L_{sc}}$ and $\theta_{0_{sc}}$ the temperature fraction could

A	λ	θ_{cyl}
A1	$\lambda 1$	0.012

Table A.2: Coefficients (censored) for the long cylinder model with Bi= conservative value and τ= value and results for the dimensionless temperature θ at r=0

be solved for the temperature of the material at middle and end position.

$\theta_{L_{sc}}$	$\theta_{0_{sc}}$
0.0094	0.0120

Table A.3: Product solutions used for the short cylinder model

Appendix B

Wall model tested for extreme values

Since the muffle edge gas temperature remains unknown, it was tested how sensitive the wall model was for temperature changes. For this, two extreme values for $T_{\infty 2}$ were inserted into the code.

At first, the highest possible edge temperature was tested, by using the exact same temperature within the muffle edges as was assumed for the furnace air. The results are displayed in figure B.1.

Secondly, an extremely low temperature was assumed as $T_{\infty 2}$, where the edge temperature would stay at room temperature for the first six time steps and afterwards always be remarkably lower than the inner furnace ambience, where the difference in $^{\circ}C$ was equal to 32% of the highest values in $T_{\infty 1}$. The corresponding graph is shown in B.2.

Both cases showed similar results as from the original test vector.

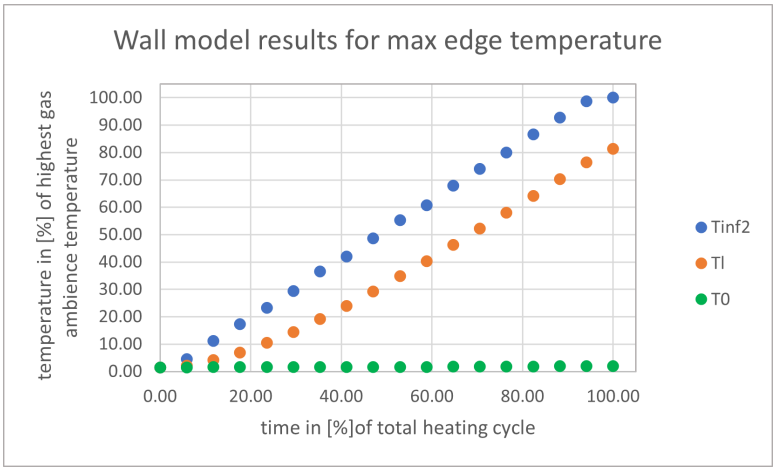

Figure B.1: Results from wall model when the inner furnace air temperature $T_{\infty 1}$ was used as $T_{\infty 2}$

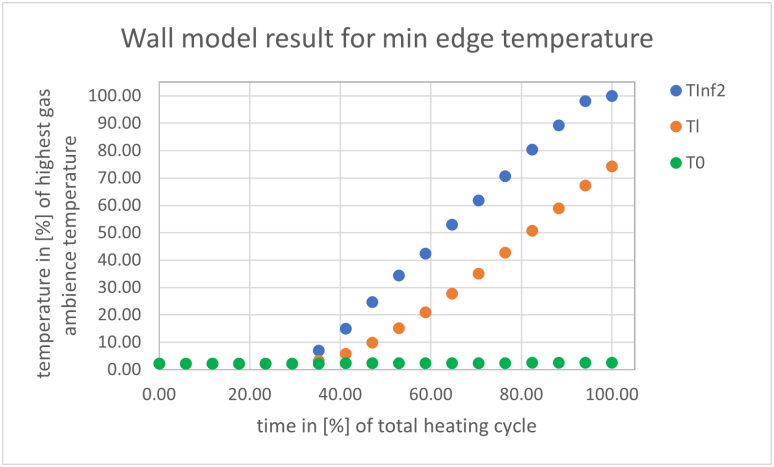

Figure B.2: Results from wall model when room the temperature was used as $T_{\infty 2}$ for the first six time steps and from thereon $T_{\infty 1}$-(value, corresponding to $T_{\infty 1_{max}} - 32\%$)

Bibliography

Richardson, David W. (2006). *Modern Ceramic Engineering*. 3rd ed. CRC Press.

Çengel, Yunus A., Robert H. Turner, and John M. Cimbala (2008). *Fundamentals of Thermal-Fluid Sciences*. 3rd ed. McGraw-Hill.

Carlström, Elis (2010). *Engineering Ceramics 2010- Introductory lecture*. Chalmers Tekniska Högskola.

Çengel, Yunus A. and Michael A. Boles (2011). *Thermodynamics- An Engineering Approach*. 7th ed. McGraw-Hill.

Biddle, John (2015). *Heat Transfer: Transient Conduction, part 2*. Last accessed 7 March 2023. URL: https://www.youtube.com/watch?v=rWy8B9kvLpc.

Incropera, Frank P. et al. (2017). *Fundamentals of Heat and Mass Transfer*. 6th ed. John Wiley Sons.

Kanthal (2021). *Kanthal joins collaborative research project into the electrification of steel production*. Last accessed 9 June 2023. URL: https://www.kanthal.com/en/news-stories/news-feed/news-media/2021/november/kanthal-joins-collaborative-research-project-into-the-electrification-of-steel-production/.

Kosky, P et al. (2021). *Exploring Engineering- An introduction to Engineering and Design (5th edition)*.

Kanthal Super Electric Heating Elements handbook (June 2022). Kanthal.

Kanthal (no date). *History*. Last accessed 27 March 2023. URL: https://www.kanthal.com/en/about-us/history/.